On the catalytic performance of open cell structures versus honeycombs

Francesco Lucci [a,*], Augusto Della Torre [b], Gianluca Montenegro [b], Panayotis Dimopoulos Eggenschwiler [a]

[a] *Laboratory for I.C. Engines, Empa, Swiss Federal Laboratories for Materials Testing and Research, Dübendorf, Switzerland*
[b] *Dipartimento di Energia, Politecnico di Milano, Milano, Italy*

ABSTRACT

Open-cell foams are increasingly gaining attention as catalytic substrates due to their promising proper-ties of high porosity, high specific surface and tortuous structure resulting in enhanced gas–wall interac-tions. However, due to the foam complex structure and variability of properties, the published data do not clarify weather true advantages of ceramic foam based catalytic converters can be expected; high gas–wall interactions may result to increased flow resistance. In the present work, foams are modelled as Kelvin Cells and compared to honeycombs, the state of the art catalyst substrates, in the controlled environment of numerical simulations. A CFD analysis has been performed assuming a mass transfer limited regime and imposing infinitive fast chemistry at the catalytic surface. Our results show that open-cell structures compared to honeycombs have higher mass transfer properties at moderate to high flow rates ($u > 2$ m/s), allowing more compact reactors. Moreover they can achieve the same conversion with a significantly lower surface, saving an equivalent fraction of noble metal. In order to have the same conversion to pressure drop trade off, foam porosity has to be much higher compared to honeycombs.

1. Introduction

In the field of catalytic converters, open-cell foams are increasingly gaining attention. They consist of a network of solid struts linked in such a way to form compacted cells. Each cell is connected to other cells through passages called windows. Their high porosity and large surface area suggest that they may have a significant advantages compared to other standard catalytic supports.

* Corresponding author.
E-mail address: francesco.lucci@empa.ch (F. Lucci).

The tortuous flow paths through the porous structures [1,2] can achieve a higher chemical activity per unit of volume compared to honeycomb reactors. However, due to the complex structure of foams and to the variability of their properties, the scientific data available in literature still do not deliver a clear assessment of foams as catalytic substrates [3–5]. Models for the geometrical characterization of the foams are still under development [6] and researchers have not yet converged in a correlation for the pressure drop that produces consistently good results [5,7,8]. A detailed investigation of the flow regimes and the consequent pressure drop through open cell foams has been proposed by Della Torre

Published Journal Article available at: http://dx.doi.org/10.1016/j.cej.2014.11.080

Nomenclature

χ	tortuosity (–)
η	conversion efficiency $\eta = \frac{C_{in}-C_{out}}{C_{in}}$ (–)
v	kinematic viscosity (m^2/s)
CPSI	Cells Per Square Inch
D	specie's diffusivity (m^2/s)
d_h	characteristic length (m^2/s)
D_p	external pore diameter $D_P = d_p + d_s = L_c$ (m)
hc	honeycomb
Hg	Hagen number $Hg = \frac{\Delta P}{\Delta x} \cdot \frac{D_h^3}{\rho \nu^2}$ (–)
KS_v	volumetric mass transfer coefficient (s^{-1})
K	mass transfer coefficient (m/s)
KC	Kelvin Cell
L_R	reactor length (m)
PPI	Pore Per Inch
r_s	reacting rate (s^{-1})
Re_p	pore Reynolds number $Re_p = \frac{D_p u}{v}$ (–)
S_w	total catalytic surface, wet surface ($S_w = S_v V$) (m^2)
Sh	Sherwood number Sh $= \frac{Kd_h}{D}$ (–)
u	inflow velocity (m/s)
Y_b	bulk molar fraction (–)
Y_s	surface molar fraction (–)
Y_X	mass fraction of specie X (–)
d_p	internal pore diameter (m)
d_s	strut diameter (m)
ε	porosity (–)
S_v	specific surface area (m^2/m^3)

et al. [33]. They investigated the flow pattern inside real and ideal foam at various Reynolds number pointing out that the main contribution to the pressure drop was given by inertial effects.

For automotive exhaust applications [10] foams supports have shown several promising advantages over standard honeycombs. The higher momentum and species exchange perpendicular to the main flow direction allows higher flow uniformity which is crucial for conversion efficiency and catalyst durability [11–13]. Their geometrical flexibility allows different reactor configurations [14]. However, compared to honeycombs, these advantages may be counterbalanced by a higher pressure drop [8].

Few works have directly compared honeycomb and foam reactors. Giani et al. [3] analysed the mass transfer of high porosity metallic foams in the mass transfer limited regime at 450 °C. Mass and momentum transfer correlations were fitted to the experimental data and compared with the honeycomb (hc) correlations. They reported that the foams can obtain the same conversion rate of honeycombs but with reactors 2.5–3 times smaller. However, the reduced size of the catalyst is balanced by an overall higher pressure drop.

Patcas et al. [4] analysed ceramic foams with low porosity $\varepsilon \backsim 75\%$ and pore size of 20 and 45 PPI. They confirmed the conclusion of Giani et al. [3] that honeycombs are more advantageous in terms of trade off conversion/pressure drop, but they highlighted that foams performs better in terms of heat transfer.

Bach and Dimopoulos Eggenschwiler [15] directly compared the two substrates in a small Diesel powered Heavy Duty truck by substituting the serial standard honeycomb catalyst with a custom foam catalyst 30% smaller. They reported that the foam catalyst performed similarly to the standard catalyst both in terms of pressure drop and conversion rate.

Recently numerical simulations have been used for detailed analysis of open cell structures [1,16–18]. Several authors have also modelled the pores of open cell foams as regular cells, [3,16,19], and even produced such structures for research [20,21] and commercial purposes [22]. In [18] the authors of the present work have analysed their open-cell structure model against real foams correlation published in literature, best results were reached with correlations obtained from real foams with high porosity and low pore count. Due to the geometrical scaling, a Kelvin Cell structure can be fully characterized by a characteristic pore dimension and its ratio with the strut diameter. However this two parameters are not sufficient to completely characterize real foams since foams with same pore count and strut diameter can have different porosity and specific surface area. This and other numerical constrains [23] limit the model and may affect the results [23,18].

In the present work we directly compare honeycombs (hc) with open Kelvin Cell (KC) structures by using the controlled environment of numerical simulations. The main purpose of the comparison is to analyse the relative advantages of each structures in terms of mass transfer and pressure drop.

2. Method

2.1. Numerical modelling and assumptions

Simulations were performed using the freely available CFD solver OpenFOAM [24]. No transient conditions are considered and the catalyst is assumed to have reached a steady state. The transport of methane CH_4 in air is simulated. A Sutherland model is applied for the transport of chemical species properties and the thermal properties are extracted from Janaf tables. The methane inflow mass concentration is $X_{CH_4} = 0.001$. In order to limit the computational load, species are assumed to have Schmidt number equal to 1. The inflow temperature is kept constant at 700 K ensuring to operate in the transport limited regime. Conjugate heat transfer between the solid and the fluid was added to the model. However the preliminary simulations showed a difference between the maximum and the minimum temperature in the solid matrix of less than 3 degrees. Thus, since the inclusion of the conjugate heat transfer greatly increases the computational costs, we choose to neglect it in the production runs and to impose a constant temperature of 750 K at the solid–fluid interface. Periodic boundary conditions are applied in the y and z directions.

Gas phase reactions are neglected. Infinitely fast heterogeneous reactions are modelled at the solid–fluid interface as boundary condition imposing a null concentration for the oxidized species (i.e CH_4). Consequently the gradient of the other chemical components is corrected on the basis of the reaction stoichiometry:

$$\frac{\partial X_i}{\partial \mathbf{n}} = \alpha_i \frac{M_i}{M_{CH_4}} \frac{\partial X_{CH_4}}{\partial \mathbf{n}} \tag{1}$$

where α_i is the stoichiometric coefficient of specie i.

2.2. Domain

In order to compare foam structures with the honeycombs, two different kinds of computational domains are built following the same procedure presented in [18].

Foams are approximated by a Kelvin Cell KC structure. A CAD-3D model is created consisting of a randomized structure of four

KCs in the flow direction and two cells in the cross flow directions. The randomization of the structure has been performed using a technique similar to [1]. The center of each cell, the relative position to the perturbed cell center of the each cell face and the relative position to the perturbed face of each cell node were randomly perturbed in all direction by as much as $0.25 * l_s$, where l_s is the strut length. The 3D model and the randomization of the structure are performed in such a way that they guarantee, at the domain boundaries, the periodicity in the cross flow directions.

A schematic of the front view of a KC is presented in Fig. 1. The main characteristic lengths sketched in Fig. 1 and the geometrical properties of the main KC structures used in the present work are summarized in Table 1. In the present study we analysed only KC with high porosities ($\varepsilon = 0.80$ and $\varepsilon = 0.90$) that lead to low pressure drop, which is a crucial factor for automotive applications. The external diameter of the cells is fixed to $D_p = 2.3$ mm corresponding to a pore density of PPI = 11. This is considered as the reference pore density. By geometrically rescaling KCs further pore densities have been considered for comparison. However, in Section 3.3.1 structures with smaller pores are analysed. Thus the KCs are geometrically rescaled to reach PPI up to 45 (see Table 3).

The specific surface area S_v for the 11 PPI structures is computed from the computational mesh and resulted in 1500 and 1150 m^2/m^3 for the cases with $\varepsilon = 0.80$ and $\varepsilon = 0.90$, respectively. These values are consistent with those reported in literature for foams of similar properties [5,6,25].

The same procedure with the different geometry was used for the hc domain. The geometry is simplified as a square channel with rounded edges, Fig. 2. A square pyramid centred with the channel was cut from the entrance and exit region to avoid excessive material accumulation due to the edge fillet, making the regions more realistic.

The schematic of the front view of a hc with the main characteristic dimensions is presented in Fig. 2. The hc structures, whose properties are summarized in Table 2, was chosen to match the properties of representative commercial honeycombs with 400 CPSI. In particular, the channel width is $D_C = 1.25$ mm and the wall thickness, including the washcoat, is assumed 0.25 mm. The resulting S_v is about 2500 m^2/m^3. Note also that in the present work the ratio between the honeycomb length and the channel width is 30, corresponding to a reactor length of about 3.7 cm. Commercial automotive reactors present a longer L_c/D_c ratio, decreasing the influence of the developing region at the channel entrance, where mass and momentum transfer are higher. In a direct comparison with the KC reactors, using a shorter reactor may slightly improve the honeycomb performance since KC structures present a very limited developing region, as shown by von Rickenbach et al. [26].

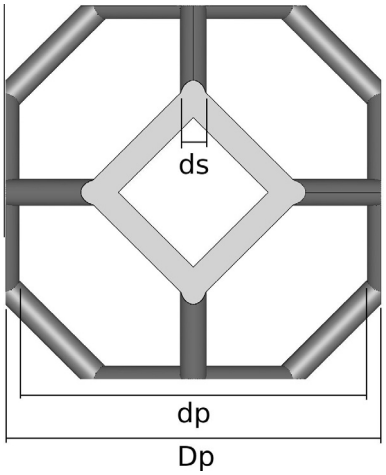

Fig. 1. Front view of KC with characteristic dimensions.

Table 1
Geometric properties of KC structures.

ε	PPI	S_v (m^2/m^3)	d_p (mm)	d_s (mm)
0.80	11	1500	1.85	0.45
0.90	11	1152	2.0	0.3

Table 2
Geometric properties of hc structure.

ε (−)	CPSI (−)	S_v (m^2/m^3)	D_c (mm)	d_c (mm)	r_c (mm)	L_c/D_c (−)
0.73	400	2480	1.25	1.125	0.375	30

Table 3
Geometric properties of KC structures obtained by geometrical scaling and used to analyse the effect of pore size.

ε	PPI	S_v (m^2/m^3)	d_p (mm)	d_s (mm)
0.80	11	1500	1.85	0.45
0.80	14	1876	1.48	0.36
0.80	22	3001	0.925	0.225
0.80	28	3751	0.74	0.18
0.80	44	6002	0.4625	0.1125
0.90	11	1152	2.0	0.3
0.90	14	1440	1.6	0.24
0.90	22	2304	1.0	0.15
0.90	28	2881	0.8	0.12
0.90	44	4609	0.5	0.075

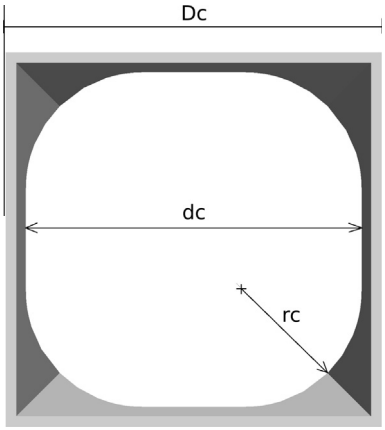

Fig. 2. Honeycomb front view with characteristic dimensions.

A visualization of the computational grid is shown in Fig. 3. For brevity sake only the entrance region of the honeycomb is presented. For both cases the mesh is of the order of 100,000s grid elements and to increase accuracy it is refined at the active catalytic surface. The final meshes are made mainly by hexahedral grid elements. The remaining elements, constituting around 10% of the total are general polyhedral elements.

3. Results and discussion

3.1. Validation

In [18] the present KC model was compared with the most common experimental correlations for real foams published in literature. Both momentum and mass transfer were analysed.

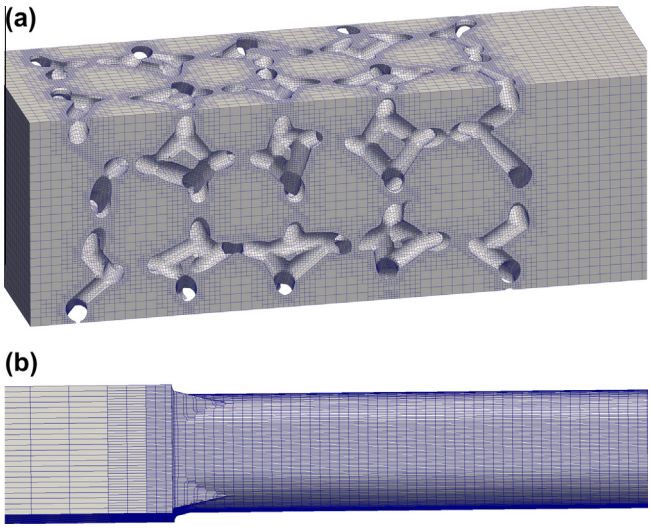

Fig. 3. Sample of the final computational grid: (a) KC structures, (b) honeycomb structures.

In the present section only the correlations of the Groppi's group [3,28] were compared to the KC model. While standard hc correlations [29] were used for the honeycomb model.

3.1.1. Sherwood number

In Fig. 4 the Sherwood number (Sh) derived from the simulations of the present work characterizes mass transfer through stacked KCs. In [18] the Sh derived from the same KC model was more extensively compared with Sh numbers for foams derived experimentally [28,5,27]. In Fig. 4, only [28] is used as reference since it is the author that analysed foams with higher porosity. Note that there is still not agreement among authors in literature and [28] reported that mass-transfer rates predicted by their correlations are 50% higher than those of his [27]. In Fig. 4 the maximum deviation between the results and the correlations is below 25%. The low porosity ($\varepsilon = 0.80$) KC model overestimates the mass transfer predicted by Groppi et al. [28]. An underestimation is obtained in the high porosity ($\varepsilon = 0.90$) case but with a maximum deviation of 10%.

Additionally, Fig. 4 shows the Sherwood numbers plotted for the honeycomb configuration, derived from the corresponding simulations of the present work and the correlation of Cybulski and Moulijn [30,29].

Note that Groppi et al.'s correlation

$$Sh^{KC} = 1.1 Re_{d_s}^{0.43} Sc^{1/3} \tag{2}$$

uses the strut diameter d_s as characteristic length scale for both the Sherwood and the Reynolds Numbers. While honeycomb correlation [4,29,30]

$$Sh^{hc} = 2.976\left(1 + 0.078 Re_{D_c} Sc \frac{D_c}{L}\right)^{0.45} \tag{3}$$

uses the channel width. Given the different geometry and length scales, comparing directly the non dimensional quantities between the two different supports may be misleading. A direct comparison can be achieved by using dimensional coefficients as it is done in Section 3.2.

3.1.2. Pressure drop

In Fig. 5 pressure gradients [Pa/mm], computed by the pressure difference between the inflow and the outflow divided by the length of the catalytic support, are plotted versus the inflow velocity.

The pressure gradients for honeycombs simulated by the present work are compared to those obtained by the Hagen–Poiseuille equation [4,29]:

$$\frac{\Delta P}{L} = \frac{32\mu}{d_c^2 \varepsilon} u. \tag{4}$$

At high velocity the present numerical model overestimate the pressure drop, compared to Eq. (4).

In Fig. 6 the pressure in the centreline of the honeycomb with inflow velocity of 10 m/s is compared with the pressure predicted by Eq. (4). The pressure drop of the present simulations agree with Eq. (4) only in the fully developer region. This is to be expected since the Hagen–Poiseuille equation, Eq. (4), assume fully developed, laminar and cold pipe flow. Only a porosity correction is added to account for the effective average velocity inside the honeycomb channel. In particular, entrance and exit effects have an inertial dependence and increases with u^2. Thus, at higher velocity higher deviations are expected as shown in Fig. 5.

KC results were compared with experimental correlations proposed by Giani et al. [31]:

$$\frac{\Delta P}{L} = \frac{2}{d_S}\left(0.87 + \frac{13.56}{Re_{d_s}}\right)\left(\frac{1}{1 - G(\varepsilon)}\right)^4 \frac{G(\varepsilon)}{4} \rho u^2 \tag{5}$$

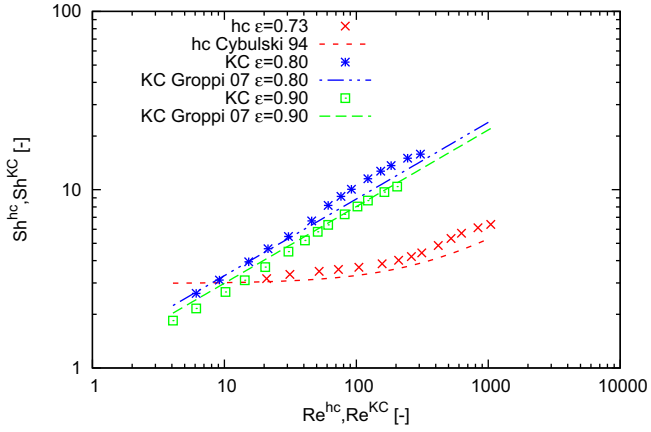

Fig. 4. Sherwood number versus Reynolds number for Kelvin Cell structures and honeycombs. Symbols: present numerical results; lines: published correlations. Here, the characteristic length for Sh and Re of the Kelvin Cells is the strut diameter, d_s, and for the honeycombs is the channel width, D_c.

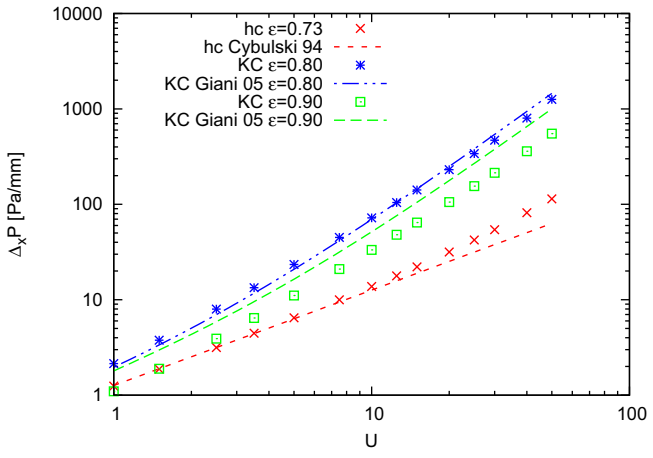

Fig. 5. Pressure drop per unit length in Pa/mm versus surface velocity.

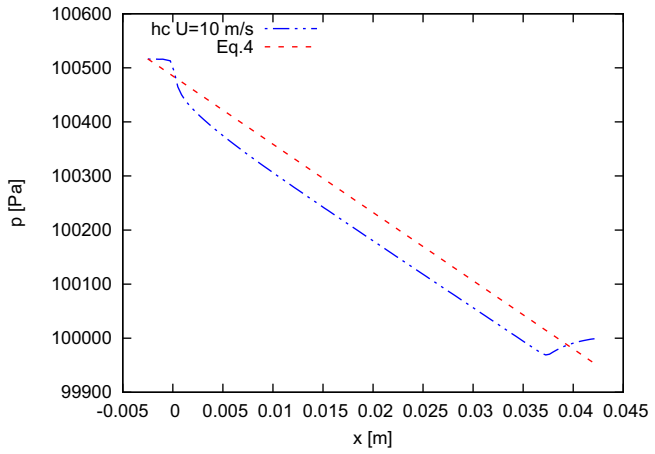

Fig. 6. Pressure in the honeycomb centreline with inflow velocity $U = 10$ m/s. Blue line represents the numerical simulation, red line the Hagen–Poiseuille equation Eq. (4). (For interpretation of the references to colour in this figure legend, the reader is referred to the web version of this article.)

where $G(\varepsilon) = 2[(1-\varepsilon)/(3\pi)]^{1/2}$.

The maximum deviation between the present results and the pressure correlation of Giani et al. is of 50%. The $\varepsilon = 80$ KC structure is predicted with a maximum deviation of approximately 10%, while the $\varepsilon = 90$ KC structure at all velocities is underestimated with a deviation that stays between 35% and 45%. Note, however, that Edouard et al. [7] in his review of the pressure correlations for open cell foams reported that no correlation currently published achieves constantly good results and variations between theoretical and experimental permeabilities of smaller than 100%, resulting in standard deviations of the predicted values respect the experimental pressure drops higher than 30%.

In Fig. 5 pressure gradients of KC structures are generally higher than those of honeycombs and have an higher dependence on the velocity. This can be seen also from correlations commonly used in the literature. In the velocity range of interest, ΔP in honeycombs varies linearly with velocity, as described by Eq. (4). In KC structures ΔP presents also an inertial term (see Eq. (5)) and it is commonly modelled by a Darcy–Forchheimer equation [27]. As a consequence, compared to honeycombs, pressure drop can become more and more a critical limiting factor for KC structures at high inflow velocities (see Fig. 5).

3.2. Mass transfer

In Fig. 4 we have already presented the Sherwood number for the honeycomb and the KC structures. However, we have already mentioned that since the geometry is different and defined by different characteristic dimensions it is not straightforward to compare the two structures. A multiple analysis is necessary to identify which catalytic support has higher performance between KC or honeycomb structures.

3.2.1. 1D transport model

By modelling the convective mass transfer from the gas region to the catalytic surface, the species equation inside the catalyst can be written as:

$$u\frac{\partial Y_b}{\partial x} = -K\ S_v\ (Y_b - Y_s) \tag{6}$$

where K is the mass transfer coefficient, S_v is the specific surface area and Y_b and Y_s are the bulk and surface molar fractions of the reacting species. In steady state regime, the catalytic reaction rate in the washcoat must be equal to the mass transfer to the surface. Thus the surface reaction rate r_s for a single step reaction can be expressed as:

$$r_s = -K\ S_v(Y_b - Y_s). \tag{7}$$

Assuming infinitely fast reactions ($Y_s = 0$), the reaction rate is:

$$r_s = -K\ S_v Y_b. \tag{8}$$

Eq. (6) with $Y_s = 0$ can be easily solved analytically. Its results can be empirically matched with the experimental data or CFD results by defining the $K\ S_v$ coefficient as:

$$KS_v = -\frac{\ln(1-\eta)}{V/Q_{in}} \tag{9}$$

where V is the catalyst volume, Q_{in} is the volumetric flow rate and η is the conversion efficiency. The Sherwood number plotted in Fig. 4 is defined as :

$$Sh = -\frac{Kd_h}{D} = \frac{ReSc}{S_v L}\ln(1-\eta) \tag{10}$$

3.2.2. Mass transfer coefficients

The KS_v coefficient for honeycombs and KC structures is plotted in Fig. 7.

From Eq. (9) it can be seen that, given a fixed flow rate Q_{in}, KS_v is inversely proportional to the volume of the reactor necessary to achieve a given conversion η. Fig. 7 shows a significantly higher KS_v value for the KC structures compared to honeycombs, implying that in similar conditions KC can achieve the same conversion rate with only a fraction of the volume required by a honeycomb.

Both KC structures at inflow velocities of 1 m/s present approximately the same KS_v coefficient of the honeycomb, but when the velocity rises to 15 m/s KC structures have more than 3 times higher KS_v coefficients, thus requiring only 1/3 of the volume to reach the same conversion.

KC structures considered in Fig. 7 have a lower specific surface S_v than honeycombs (see Tables 2 and 1). Thus, combined with the lower volume, they require also a lower total catalytic surface ($S_w = S_v V$).

This is visualized in Fig. 8 where the mass transfer coefficient K is plotted. Similarly to the KS_v coefficient, K is inversely proportional to the needed wet surface S_w, and can be expressed as:

$$K = -\frac{\ln(1-\eta)}{S_w/Q_{in}}. \tag{11}$$

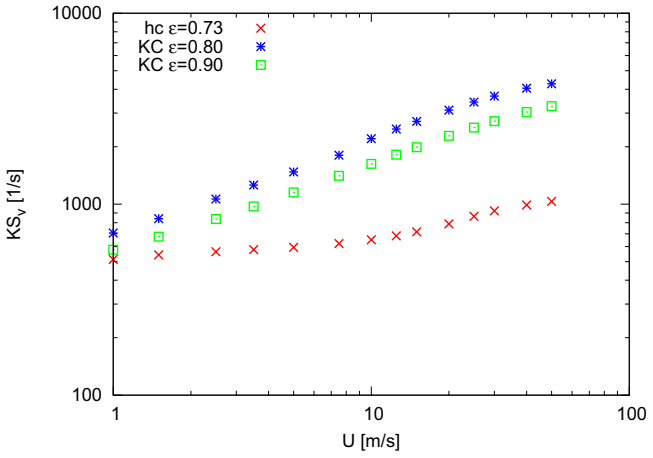

Fig. 7. $K\ S_v$ coefficient versus inflow velocity.

KC structures, even at low velocity (1 m/s), have approximately double mass transfer coefficient K, outperforming the honeycomb structures. Thus, already at low velocities (≈ 1 m/s) it needs half of the surface to obtain the same conversion rate. This surface gain improves at higher velocities.

Assuming the same washcoat properties and washcoat thickness for both supports, the total amount of noble metal used in the reactor is proportional to the total wet surface S_w. The use of a support that minimizes the total surface needed, minimizes the amount of noble metal required.

In Fig. 9 shows the ratios of the total catalytic surface and volume of the KC reactors to those required to achieve the same conversion with honeycombs. With increasing flow velocity, KC structures need a smaller fraction of the honeycomb surface and volume. Due to the domain dimensions, after $U \approx 10$ m/s entry-region effects become more and more important in the honeycomb improving its transfer properties and causing the ratios in Fig. 9 to stabilize.

It has to be noted that this estimation considers only the species transport to the surface due to external diffusion and convection. The lower surface required by the KC structures is an indication of the higher transport fluxes that they are able to guarantee to the surface. However, these higher external fluxes in reality may be limited by washcoat diffusion or by chemical kinetics that have been neglected in the present simulations. The inclusion of these limitations may consequently reduce the relative advantage of KC structures over honeycombs.

3.3. Pressure/conversion trade off

Giani et al. [3] defined a dimensionless performance index as:

$$I = \frac{-\ln(1-\eta)}{\Delta P/(\rho u^2)}. \tag{12}$$

Structures with higher index give a higher ratio between conversion rate and pressure drop.

The indexes I for each set of simulations are plotted in Fig. 10. As already reported in [18] I increases with the porosity. KC structure with porosity $\varepsilon = 0.9$ perform similarly to the honeycomb with $\varepsilon = 0.73$.

Previous comparisons of foams and honeycombs as catalytic supports, presented by Giani et al. [3] and Patcas et al. [4], predicted a lower performance index for foams compared to honeycombs.

Patcas et al. focused on comparing foams and honeycombs with approximately the same specific surface area. This resulted in analysing foams with lower porosity ($\varepsilon \backsim 0.74$) than the one considered in the present work. For the honeycomb of $\varepsilon = 0.7$ they reported an I of approximately $I \backsim 0.2$ which is consistent with our results in Fig. 10. For the foam they reported an I of approximately $I \backsim 0.05$. Our model predicts (not shown here) for KC structures with porosity $\varepsilon = 0.73$ a I of approximately of $I \backsim 0.1$ until inflow velocities of $U = 10$ m/s and only at higher velocity I decreases below 0.1. The difference can be explained by the fact that Patcas et al. used in the analysis foams with low porosity and high PPI. Such structures deviates from the ideal KC structures used in the present work, due to the excessive material accumulation at the cell nodes, to the non uniform cross section of the struts and to the increased frequency of closed windows.

The results of the present simulations are more consistent with the work of Giani et al. [3] which analysed foams with high porosity and low PPI. Compared to the present work, [3] predicts a slightly higher performance index for the honeycomb and an slightly lower index for foams with even higher porosity ($\varepsilon \backsim 0.95$). The present simulations overall confirm the result of [3], but they suggest also that properly designed foams with high enough porosity may have the performance index I in the same range of commercially available honeycombs.

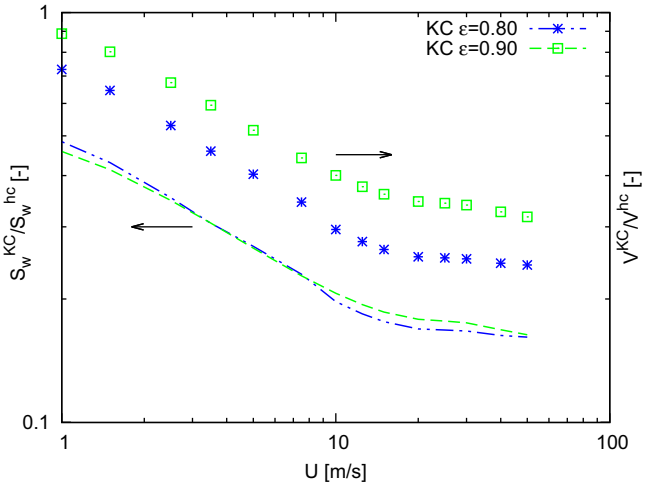

Fig. 9. Ratios of the total catalytic surface (symbols) and reactor volume (lines) of the KC reactors to those required to achieve the same conversion in the honeycombs.

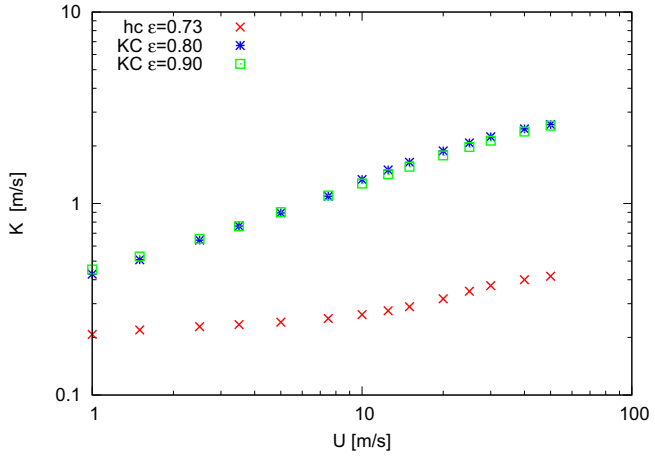

Fig. 8. Mass transfer coefficient versus inflow velocity.

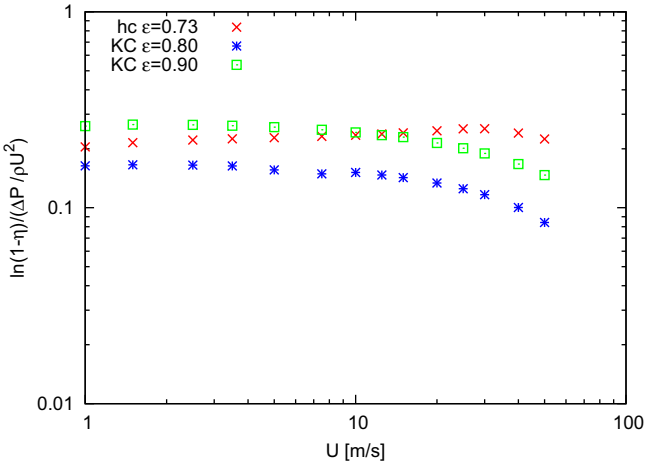

Fig. 10. Performance coefficient I (Eq. 12) versus inflow velocity.

3.3.1. Pore size effect on pressure/conversion trade off of Kelvin Cells

Lucci et al. [18] showed that for KC structures the performance index I of the scales with the porosity and the Reynolds Number Re_p, and peaks around $Re_p = 70$ [18]. Thus, after having maximized the porosity, for best performance the pore size of the KC structures should be sized so the Re_p is about 70.

In this section structures presented in 2.2 are geometrically rescaled in order to compare structures with different pore density. Note that, for the properties of the geometrical rescaling the porosity stays constant and the specific surface area is inversely proportional to the scaling factor. Thus doubling the pore diameter will reduce S_v by half. An overview with the geometrical properties of the KC structures obtained can be found in Table 3. In Fig. 11 the index I of these structures is plotted versus the inflow velocity.

For both porosities $\varepsilon = 0.80$ and 0.90, at velocities lower than 5 m/s the structures with PPI = 11 are the most efficient, while at higher velocities the 44 PPI structure become more efficient in terms of pressure/conversion ratio. This result is clearly a consequence of the Reynolds number scalability of reactor set up as discussed by Lucci et al. [18]. Observed for fast reactions, it has yet to be verified in real foams under regimes controlled by reaction speed or washcoat diffusion.

3.3.2. Dimensional performance index

The index I is best suited to compare foams and honeycombs in the same configuration and with the same inflow velocity, because it is non-dimentionalized by (ρu^2) (see Eq. (12)). However, compared to honeycombs, foams have higher geometrical versatility and allow more flexibility in designing the reactor geometrical configuration [14]. The geometry of the reactor can drastically change the flow, and so one may be interested in comparing the performance of the two structures operating under different flow conditions.

In Fig. 10, the value of the performance index I is relatively constant $(0.1 < I < 0.3)$ trough the all range of velocity considered $(1 < U < 50)$. This implies that, the conversion rate η for a given pressure drop, will decrease by decreasing the inflow velocity according to $-\ln(1-\eta)/\Delta P \propto 1/u^2$ (see Eq. (12)), explaining the advantage of configurations that maximise the cross section area in order to minimize the average flow velocity.

The index I_p is the ratio of the conversion rate per unit of length and the pressure gradient. It is equivalent to the performance index I divided by ρu^2:

$$I_p = \frac{-\ln(1-\eta)}{\Delta P}. \tag{13}$$

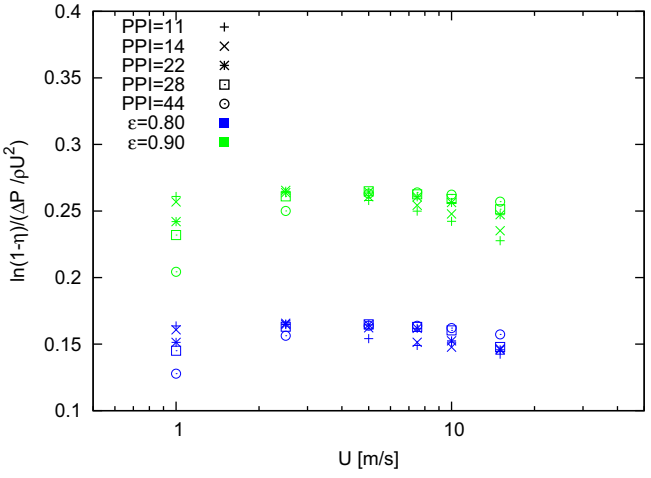

Fig. 11. Performance coefficient I (Eq. 12) versus inflow velocity for KC structures with different pore count ($11 < \text{PPI} < 44$) and two porosities $\varepsilon = 0.80$ and 0.90.

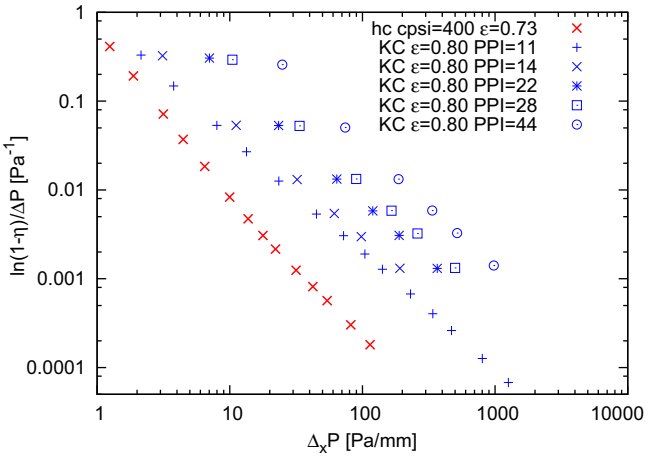

Fig. 12. Dimensional performance coefficient I_p (Eq. 13) versus pressure gradient.

In Fig. 12 the dimensional performance coefficient I_p is plotted versus the pressure gradient.

From the figure it is clear that, for a given pressure gradient, the KC structures considered are able to achieve higher conversions if compared to honeycombs. The main reason, is that in the KC structures, a given pressure gradient is reached at lower velocities (Fig. 5) where the conversion is more efficient.

In Fig. 12 also the I_p for structures with different pore density are plotted. On one side, increasing the PPI significantly increases the pressure gradient but the performance index I_p stays relatively stable. On the other side, the same pressure gradient can be reached by structures with higher pore count operating at lower velocities where the index I_p is higher.

These considerations are significant for those applications where the length in the flow direction is limited. In this case, once the pressure drop has been maximised to the maximum allowed the only structures that can guarantee a given level of conversion may be KC structures with high pore density.

4. Conclusions

In this study we perform a comparison between Kelvin cell and honeycomb structures as a support for catalytic reactors. CFD simulations of both structures where performed to investigate their momentum and mass transfer properties. The structures were assumed to be at a high enough temperature to operate in a mass transfer limited regime. Thus, infinitely fast reactions were assumed at the catalytic surface and washcoat diffusion was neglected.

The main conclusions and achievements of the work are:

- Both Kelvin Cell and honeycomb models follow the trends of published correlations [3,29]. The differences observed are justified by the idealization of the geometry or to the physical assumption made.
- Compared to honeycomb, with few exceptions, KC structures are able to deliver higher momentum and mass transfer properties for the inflow velocity and for the geometrical configuration considered.
- The higher mass transfer properties of KC structure allow to reach the same conversion rate of honeycombs with only a fraction of the volume or of the catalytic surface. In particular, in the velocity range considered, the catalytic surface required by the KC structure is at least half the one of honeycomb. This is expected to save an equivalent fraction of noble metal.

- KC structure present a higher velocity dependence in both pressure and mass transfer correlations. However, for high porosity structures, the performance index I peaks at around $Re_p = 70$ indicating an optimal operational range, where the structures are more efficient in terms of pressure/conversion trade off.
- The porosity of the KC structure will determine whether the KC has an higher performance index compared to honeycomb.

Acknowledgments

The authors gratefully acknowledge financial support from Swiss Kompetenzzentrum für Energie und Mobilität CCEM via Project Number 704 and from the Italian Ministry of Education, University and Research, Rome (MIUR, Progetti di Ricerca Scientifica di Rilevante Interesse Nazionale, prot. 2010XFT2BB), within the project IFOAMS: Intensification of Catalytic Processes for Clean Energy, Low-Emission Transport and Sustainable Chemistry using Open-Cell Foams as Novel Advanced Structured Materials.

References

[1] P. Habisreuther, N. Djordjevic, N. Zarzalis, Statistical distribution of residence time and tortuosity of flow through open-cell foams, Chem. Eng. Sci. 64 (23) (2009) 4943–4954.
[2] A.J. Onstad, C.J. Elkins, F. Medina, R.B. Wicker, J.K. Eaton, Full-field measurements of flow through a scaled metal foam replica, Exp. Fluids 50 (6) (2011) 1571–1585.
[3] L. Giani, G. Groppi, E. Tronconi, Mass-transfer characterization of metallic foams as supports for structured catalysts, Ind. Eng. Chem. Res. 44 (14) (2005) 4993–5002.
[4] F. Patcas, G. Garrido, B. Kraushaar-Czarnetzki, CO oxidation over structured carriers: a comparison of ceramic foams, honeycombs and beads, Chem. Eng. Sci. 62 (15) (2007) 3984–3990.
[5] G. Incera Garrido, F. Patcas, S. Lang, B. Kraushaar-Czarnetzki, Mass transfer and pressure drop in ceramic foams: a description for different pore sizes and porosities, Chem. Eng. Sci. 63 (21) (2008) 5202–5217.
[6] A. Inayat, H. Freund, T. Zeiser, W. Schwieger, Determining the specific surface area of ceramic foams: the tetrakaidecahedra model revisited, Chem. Eng. Sci. 66 (6) (2011) 1179–1188.
[7] D. Edouard, M. Lacroix, C. Huu, F. Luck, Pressure drop modeling on SOLID foam: state-of-the art correlation, Chem. Eng. J. 144 (2) (2008) 299–311.
[8] P. Dimopoulos Eggenschwiler, D. Tsinoglou, J. Seyfert, C. Bach, U. Vogt, M. Gorbar, Ceramic foam substrates for automotive catalyst applications: fluid mechanic analysis, Exp. Fluids 47 (2) (2009) 209–222.
[9] A.Della TorreG.MontenegroG.TaborM.WearsCFD characterization of flow regimes inside open cell foam substratesInt. J. Heat Fluid Flow (0).
[10] M. Twigg, Progress and future challenges in controlling automotive exhaust gas emissions, Appl. Catal. B 70 (1–4) (2007) 2–15.
[11] G. Gaiser, J. Oesterle, J. Braun, P. Zacke, The progressive spin inlet - Homogeneous flow distributions under stringent conditions, SAE Technical Papers.
[12] A.P. Martin, N.S. Will, A. Bordet, P. Cornet, C. Gondoin, X. Mouton, Effect of flow distribution on emissions performance of catalytic converters, SAE Technical Papers.
[13] K. Zygourakis, Transient operation of monolith catalytic converters: a two-dimensional reactor model and the effects of radially nonuniform flow distributions, Chem. Eng. Sci. 44 (9) (1989) 2075–2086.
[14] G.C. Koltsakis, D.K. Katsaounis, Z.C. Samaras, D. Naumann, S. Saberi, A. Böhm, I. Markomanolakis, Development of metal foam based aftertreatment system on a diesel passenger car, SAE Technical Papers (2008-01-0619).
[15] C. Bach, P. Dimopoulos Eggenschwiler, Ceramic foam catalyst substrates for diesel oxidation catalysts: Pollutant conversion and operational issues, SAE Technical Papers (2011-24-0179).
[16] K. Boomsma, D. Poulikakos, Y. Ventikos, Simulations of flow through open cell metal foams using an idealized periodic cell structure, Int. J. Heat Fluid Flow 24 (6) (2003) 825–834.
[17] E. Bianchi, T. Heidig, C.G. Visconti, G. Groppi, H. Freund, E. Tronconi, An appraisal of the heat transfer properties of metallic open-cell foams for strongly exo-/endo-thermic catalytic processes in tubular reactors, Chem. Eng. J. 198–199 (2012) 512–528.
[18] F. Lucci, A. Della Torre, J. von Rickenbach, G. Montenegro, D. Poulikakos, P. Dimopoulos Eggenschwiler, Performance of randomized Kelvin cell structures as catalytic substrates: mass-transfer based analysis, Chem. Eng. Sci. 112 (2014) 143–151.
[19] A. Inayat, J. Schwerdtfeger, H. Freund, C. Körner, R. Singer, W. Schwieger, Periodic open-cell foams: pressure drop measurements and modeling of an ideal tetrakaidecahedra packing, Chem. Eng. Sci. 66 (12) (2011) 2758–2763. T.
[20] Knorr, P. Heinl, J. Schwerdtfeger, C. Körner, R.F. Singer, B.J. Etzold, Process specific catalyst supports—selective electron beam melted cellular metal structures coated with microporous carbon, Chem. Eng. J. 181–182 (2012) 725–733.
[21] M. Klumpp, A. Inayat, J. Schwerdtfeger, C. Körner, R.F. Singer, H. Freund, W. Schwieger, Periodic open cellular structures with ideal cubic cell geometry: effect of porosity and cell orientation on pressure drop behavior, Chem. Eng. J. 242 (2014) 364–378.
[22] A. Ortona, C. D'Angelo, S. Gianella, D. Gaia, Cellular ceramics produced by rapid prototyping and replication, Mater. Lett. 80 (2012) 95–98.
[23] Z. Wu, C. Caliot, G. Flamant, Z. Wang, Numerical simulation of convective heat transfer between air flow and ceramic foams to optimise volumetric solar air receiver performances, Int. J. Heat Mass Transfer 54 (789) (2011) 1527–1537.
[24] www.openfoam.org.
[25] J. Grosse, B. Dietrich, G. Incera Garrido, P. Habisreuther, N. Zarzalis, H. Martin, M. Kind, K.-C. Bettina, Morphological characterization of ceramic sponges for applications in chemical engineering, Ind. Eng. Chem. Res. 48 (23) (2009) 10395–10401.
[26] J. von Rickenbach, F. Lucci, C. Narayanan, P.D. Eggenschwiler, D. Poulikakos, Multi-scale modelling of mass transfer limited heterogeneous reactions in open cell foams, Int. J. Heat Mass Transfer 75 (2014) 337–346.
[27] J. Richardson, Y. Peng, D. Remue, Properties of ceramic foam catalyst supports: pressure drop, Appl. Catal. A 204 (1) (2000) 19–32.
[28] G. Groppi, L. Giani, E. Tronconi, Generalized correlation for gas/solid mass-transfer coefficients in metallic and ceramic foams, Ind. Eng. Chem. Res. 46 (12) (2007) 3955–3958.
[29] A. Cybulski, J. Moulijn, Monoliths in heterogeneous catalysis, Catal. Rev. – Sci. Eng. 36 (1994) 179–270.
[30] R. Hawthorn, Afterburner catalysts effects of heat and mass transfer between gas and catalyst surface, Amer. Inst. Chem. Engns. Symp. Ser. 70 (137) (1974) 428–438.
[31] L. Giani, G. Groppi, E. Tronconi, Heat transfer characterization of metallic foams, Ind. Eng. Chem. Res. 44 (24) (2005) 9078–9085.